In-situ observations of the fracture and adhesion of Cu/Nb multilayers on polyimide substrates

M.J. Cordill[1*], A. Kleinbichler[1], B. Völker[1+], P. Kraker[1], D.R. Economy[2++], D.M. Többens[3], C. Kirchlechner[4], M.S. Kennedy[2]

[1] Erich Schmid Institute of Materials Science, Austrian Academy of Sciences, and Department of Material Physics, Montanuniversität Leoben, Jahnstrasse 12, Leoben 8700, Austria

[2] Department of Materials Science & Engineering, Clemson University, Olin Hall, Clemson, SC 29634 USA

[3] Helmholtz-Zentrum Berlin für Materialien und Energie (HZB), Albert-Einstein-Str. 15, 12489 Berlin, Germany

[4] Max-Planck-Institut für Eisenforschung GmbH, Max-Planck-Str.1, 40237 Düsseldorf, Germany

[+]Now at: Materials Chemistry, RWTH Aachen University, Kopernikusstrasse 10, 52074, Germany

[++]Now at: Micron Technology Inc., Technology Development, Boise, ID, 83707, USA

Abstract

Cu/Nb nanoscale metallic multilayers have been extensively investigated to understand how their mechanical behavior is influenced by the individual layer thickness. The general observed trend is that the yield stress of the multilayer increases with decreasing layer thickness. Important mechanical behaviors that have not been studied in-depth are the fracture and adhesion energy between the film and substrate. Here, the influence of the layer thickness, layer order, and initial residual stresses of Cu/Nb multilayers on polyimide were examined using in-situ x-ray diffraction and confocal laser scanning microscopy under tensile loading. With these techniques, it was possible to calculate the stresses developing in the individual materials and measure buckles that could be used to evaluate the interfacial adhesion. Layer thickness, deposition order, and the initial residual stresses were not shown to influence the initial fracture strains of the Cu/Nb multilayer systems. However, the adhesion energy between the multilayer and substrate was affected by the layer deposition order and by the initial residual stresses.

Introduction

Nanoscale metallic multilayers (NMMs), or layered composite geometries where the constituents are sub-100 nm metallic layers, have been a recent interest in research primarily due to their novel strengthening behavior [1]. As the NMM characteristic length (e.g. layer thickness) decreases below ~75 nm, strength deviates from traditional theories such as Hall-Petch [2–4]. NMMs can be found in many places ranging from pearlite in steels [5] to engineered coatings, foils, and films [6,7]. These systems are being explored as wear-resistant coatings [8,9], high-strength foils [10], and radiation resistant composites [11], among others. It has been observed that freestanding Cu-based NMMs, using a variety of techniques, undergo ductile failure with very little necking prior to fracture and the yield stress increases as the individual layer thickness decreases [12–15]. However, when NMMs are deposited onto polymer substrates and strained under tension, the behavior is considered very brittle with very little observable strengthening [16–18]. When the tensile straining is performed in-situ with x-ray diffraction (XRD), the strengthening of the ductile phase and load sharing of the Cu layers was observed [19]. It is advantageous to use in-situ XRD methods because it is possible to measure the residual and mechanical response of both NMM materials under tensile loading. For example, Cu and Nb have strong reflecting peaks that are within 10° of one another and these peaks can be captured simultaneously during in-situ straining using the $\sin^2\Psi$ method to measure the lattice strain of each material. This in-situ straining method has been shown to be very valuable to study the role of film thickness, interlayers and residual stresses of metal films on polymer substrates [19–24]. Another in-situ method is to strain while imaging with a confocal laser scanning microscope (CLSM) [25,26]. The advantage of CLSM is that 3-dimensional (3D) images of the surface are created, which allow the evaluation of cracking, deformation and delamination of the films as a function of strain [25–28]. The dimensions of the delamination buckles can be used to quantitatively calculate the interface strength [20,29,30]. The focus of this study was to examine the role of thickness, layer order and initial residual stresses of the Cu and Nb layers on the fracture and interface behavior of these films using advanced in-situ XRD and CLSM techniques. The combination of these advanced methods provides a more in-depth look at the mechanical and interfacial behavior of NMMs on polymer substrates.

Experimental

Cu/Nb multilayers were deposited onto 50 μm thick Upilex® polyimide (PI) using direct current (DC) magnetron sputtering. Four different multilayer samples were made by

varying the layer thicknesses between 20 nm and 100 and altering the deposition order of the layers onto the PI (Cu or Nb in direct contact with the PI) [31]. For simplicity, the following convention is used to identify the samples: the first material in the sample name is the film that was deposited no to the substrate first to a thickness of either 20 or 100 nm. Therefore, the four samples under investigation were CuNb20, CuNb100, NbCu20 and NbCu100. All samples had a total thickness of ~950 nm, with the exception of the NbCu100. The NbCu100 film only had a thickness of ~750 nm due to the deposition of 50 nm Cu layers instead of 100 nm layers (Table I).

Synchrotron radiation (KMC-2 beamline [32], BESSY II, Berlin) was used to measure the lattice strains of the Cu and Nb layers in-situ using XRD and the $\sin^2\Psi$ method [33]. The longitudinal Cu and Nb lattice strains (parallel to the tensile direction) were measured in-situ during continuous straining with an Anton Paar TS600 to a maximum engineering strain of 12% using a displacement rate of 1 µm/s. All XRD measurements were performed in the in reflection geometry. The (111) reflections of the Cu layer and the (110) Nb reflections were recorded simultaneously with a Bruker VÅNTEC 2000 detector using five different Ψ angles between 0 and 50 degrees, using an exposure time of 10 s and a beam wavelength of 0.177 nm (spot size 300 µm). Before and after straining, high resolution measurements using 11 different Ψ angles were performed to determine the initial and final stresses in the Cu and Nb layers. A Pearson fit was applied to determine peak positions and peak widths. Film stresses were calculated using x-ray elastic constants (XECs) ($1/2\ S_2$) [34] for untextured (111) Cu and (110) Nb reflections. XECs were calculated from single-crystal elastic constants assuming the Hill model with the software ElastiX [35].

For comparison and to assess the adhesion energies, in-situ CLSM straining was performed using the same tensile device on an Olympus LEXT 4100 OLS. The Cu/Nb multilayers were strained with stepwise loading in order to image the surface during straining. Initially, small steps were utilized (e.g. 0.1%, 0.25%, 0.5% strain) to observe the initial fracture strain, ε_f. After cracks were observed, larger steps were employed (1-2% strain increments) until the maximum strain of 12%. The in-situ CLSM experiments were run at 10 µm/s. Using CLSM has the advantage of 3D surface imaging of large areas in short times. Each image made during in-situ straining needed about 2 min and if delamination occurred, the buckles could be used to evaluate the interface adhesion without additional experiments [25,29]. At least two in-situ CLSM experiments were performed in order to get some statistics on the ε_f. Post imaging of all samples was performed with scanning electron microscopy (SEM) and cross-sectional

focused ion beam (FIB) milling to confirm the layer order, total multilayer film thicknesses (Figure 1) and to confirm the failing interfaces (Nb-PI or Cu-PI).

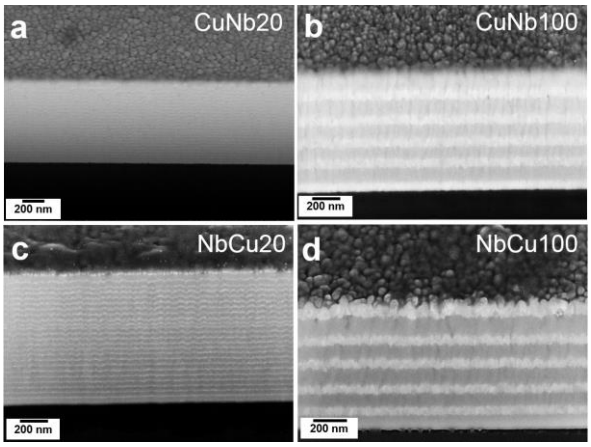

Figure 1: FIB cross-sections of the multilayer films, (a) CuNb20, (b) CuNb100, (c) NbCu 20 and (d) NbCu100.

Results and Discussion

Initially, the stresses in the Cu and Nb layers are thickness dependent (Table I). The 20 nm Cu layers have residual tensile stresses on the order of 1 GPa, while the 100 nm Cu layers are on the order of 200-700 MPa tensile. A similar trend is observed in the Nb layers with the 20 nm layers also having residual stress greater than 1 GPa tensile. However, the 100 nm Nb layers have compressive residual stresses of -500 MPa. With the residual stresses being generally tensile, it is expected that the films will fail at low strains [24]. The initial residual stresses of all samples are shown in Figure 2 as the first data point at an engineering strain of 0%.

Measurement of the lattice strains and calculation of stresses of the Cu and Nb layers provides vital information about the mechanical behavior. From previous studies the shape of the measured film stress as a function of engineering strain is well understood [20,23,36,37]. Initially the stress increases elastically until a maximum stress is reached. The strain at which the maximums stress is achieved is considered to be the fracture strain where through thickness cracks initiate in brittle film systems. After reaching the maximum stress, the stress decreases due to continued crack formation until a stress plateau is attained. The stress plateau is indicative of crack density saturation where no new cracks form. Upon unloading from 12% strain, the film stress decreases as the polyimide substrate recovers elastically.

As shown in Figure 2, the samples made of 20 nm layers all had higher stresses compared to the samples made with 100 nm layers during straining. Both layer orders are also within the same stress range and the 100 nm Nb layers remain compressive even at 12% of

strain. The results of Figure 2 demonstrate that the individual layer thickness is the main parameter that dominates the stress carrying behavior in multilayers, as has been previously discussed [13,15,19]. Since the 20 nm layers achieve higher stresses before and during straining, they follow the "smaller is stronger" theory quite well [14]. The results also mirror those of Polyakov et al. [19], demonstrating an increased maximum stress with decreasing layer thickness and possible load sharing within the layers. The strain that the maximum stresses are reached is a little under 1% for all samples. It should be noted that the measured stresses in the 100 nm layers are more scattered. When Nb is the first layer, the Cu layers achieved slightly higher stresses than when Cu was the first layer. Recall that in the NbCu100 sample the Cu layer is thinner than the CuNb100 sample. FIB cross-sectioning (Figure 1d) confirmed that the Cu layers are on average 50 nm thick and the Nb layers are about 75 nm. The difference in thickness is the most likely reason for the different maximum stresses [19].

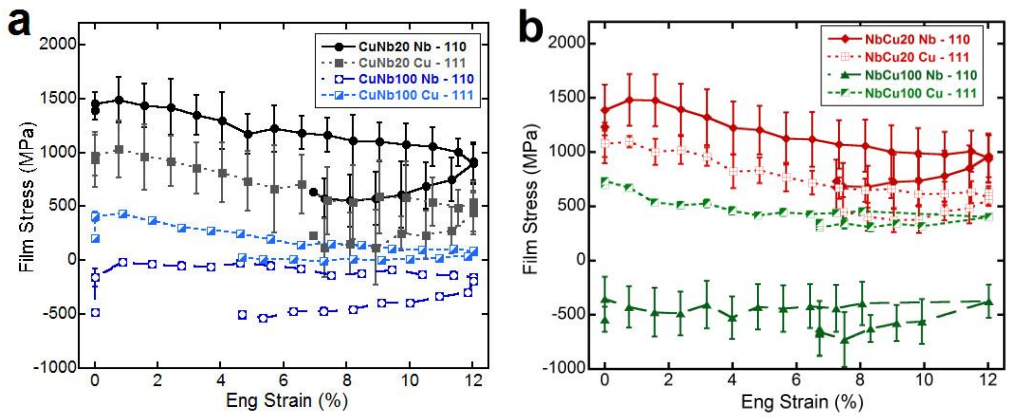

Figure 2: Film stress as a function of engineering strain for the 20 nm and 100 nm multilayers with (a) CuNb layer order and (b) NbCu layer order. Error bars are calculated by the standard deviation of the peak positions.

The initial fracture strains, ε_f, and initial buckling strains, ε_b, of the multilayer films were observed during the in-situ CLSM experiments. All films crack at strains below 1%, similar to the in-situ XRD experiments (Table I). The crack density evolution of the multilayer films is shown in Figure 3 and illustrates that the crack saturation was reached for the multilayers between 6-8% strain. Of interest is that the 20 nm multilayers (CuNb20, NbCu20) have a larger saturation crack spacing (lower crack density) than the 100 nm multilayers (CuNb100, NbCu100). At 12% maximum strain the average saturation crack spacing for the 20 nm multilayers is 45 µm and for the 100 nm multilayers almost half at 25 µm (Figure 4). Normally for single layer films, thinner films have a smaller crack spacing (higher density) than thicker films of the same material [38–41]. It can also be observed that the layer order only has a small

effect on the ε_f, with CuNb fracturing at about 0.3% strain and NbCu at approximately 0.5% strain.

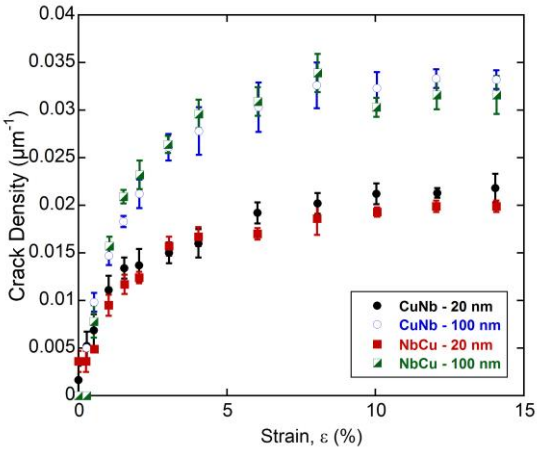

Figure 3: Crack density evolution from the in-situ CLSM experiments. The NMMs with 20 nm layers have a lower crack density than those with 100 nm layers.

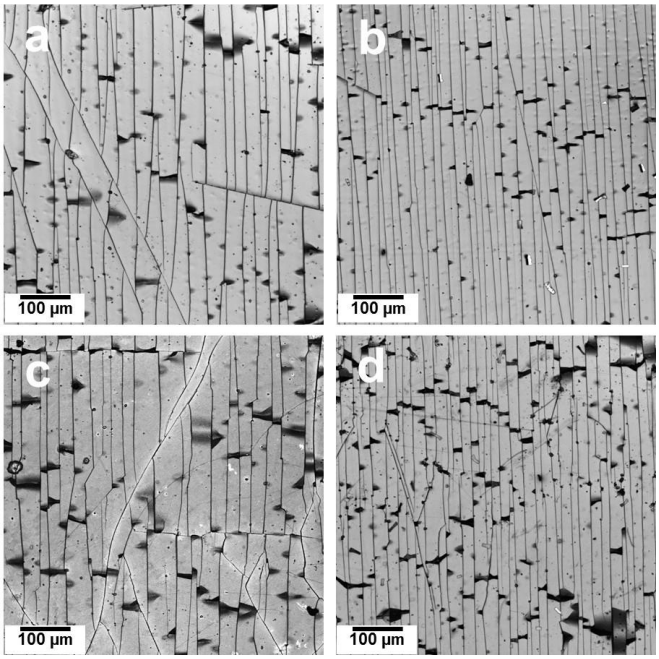

Figure 4: CLSM laser images of the Cu/Nb multilayers strained to 12% illustrating the difference in the crack density as a function of layer thickness; (a) CuNb20, (b) CuNb100, (c) NbCu20, and (d) NbCu100. Buckles are parallel to the straining direction (arrow).

Buckling of the films begins at different levels of strains for each film system depending on the layer thickness, order and residual stresses in the Nb and Cu layers. The films which start with Cu buckle between 4-6% strain while the multilayers that begin with Nb buckle as early as 2% strain. The lowest observed buckling strain of the NbCu100 could be due to the 540 MPa compressive residual stress that is present in the Nb layers compared to the 1.2 GPa tensile stress in the 20 nm Nb layers. The presence of residual compressive stresses normal to the strain direction in the Nb could cause early bucking. This would be similar to Mo films with a residual

tensile strain and fracturing at extremely low strains when loaded in tension compared to films of the same thickness having a compressive residual stress. A ε_f gain of a factor of six was found by tuning the residual stress [24]. In the case of buckling, a high compressive stress would indicate that less tensile strain is needed to induce enough compressive strain to cause buckling. Another reason for the lower buckling strains is simply that Nb and PI do not form a strong bond when sputter deposited onto PI, while Cu-PI can form a strong interface [42]. However, it should be noted that observation of the buckling strains is somewhat subjective because the in-situ CLSM measurements are very localize and concentrate on only one area of the sample.

From the buckles which form at the buckling strains and at higher strains the adhesion energy for the different metal-polymer interfaces can be calculated [25,43]. Buckle dimensions were measured from the CLSM height images starting at the buckling strain. In order to have enough buckles for good statistics within one experiment, newly formed buckles at higher strains were also included in the calculation. An example of the buckle measurements at different strains for the NbCu100 system is shown in Figure 5. Buckles with a round and symmetric shape (Figure 5 insets) are also preferred for the model [43–45].

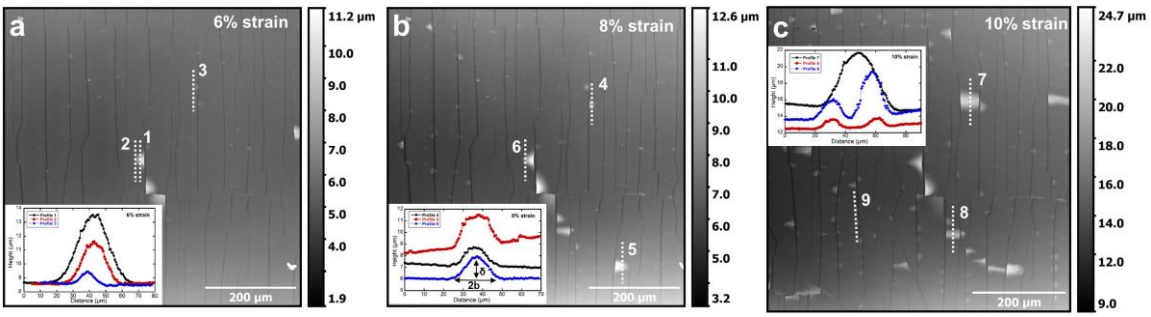

Figure 5: CLSM height images from a NbCu100 in-situ experiment at (a) 6% strain, (b) 8% strain, and (c) 10% strain illustrating how the buckle dimensions were measured for the adhesion calculation (inset b).

To calculate the adhesion energy, the buckle height, δ, and half-buckle width, b, are normalized with total films thickness, h. The values are then plotted as $(\delta/h)^{1/2}$ versus (b/h) and the equation [43]

$$\left(\frac{\delta}{h}\right)^{\frac{1}{2}} = (2\propto)^{\frac{1}{4}}\left(\frac{b}{h}\right)\left[1+\sqrt{1+\frac{3}{4}\propto\left(\frac{b}{h}\right)^{4}}\right]^{-\frac{1}{4}} \quad (1)$$

is fitted using the parameter α. The minimum α-value is used to characterize the buckle data and the adhesion energy is calculated as:

$$\Gamma = \frac{\alpha h E\prime}{4}\left(\frac{\pi}{2}\right)^{4}. \quad (2)$$

In Eqn. (2) $E' = E/(1-\upsilon^2)$ with E the elastic modulus of the thin film system (135 GPa for CuNb or NbCu [31]) and υ is the Poisson's ratio of the film (0.35). For the CuNb film data (Figure 6a) can be fit with α = 5 x 10^{-5}, which yields an adhesion energy of 10.7 ± 2.1 Jm^{-2} for the Cu-PI interface. The NbCu20 yielded an adhesion energy of 6.3 ± 2.1 Jm^{-2} with α = 3x10^{-5} and the NbCu100 a somewhat lower value of 1.4 ± 0.2 Jm^{-2} with α = 8 x 10^{-6} (Figure 6b). The difference between the two Nb-PI interfaces (Table I) is most likely due to the high compressive residual stress in the 100 nm Nb layers. The layer order should lead to a difference in interface adhesion energies and the fact that the more ductile Cu layer has a higher adhesion energy than the brittle Nb layer fits well with values available in the literature. For example, adhesion energies for Cr, Ti, or Mo on PI are usually around 5 Jm^{-2} and lower [40,43,46] while adhesion energies for Al or Au on PI can be as high as 30 Jm^{-2} [25,30]. The multilayer architecture also demonstrates that combining ductile an brittle layers, ductile materials will become brittle and interface fracture is more likely to occur [20,26,47].

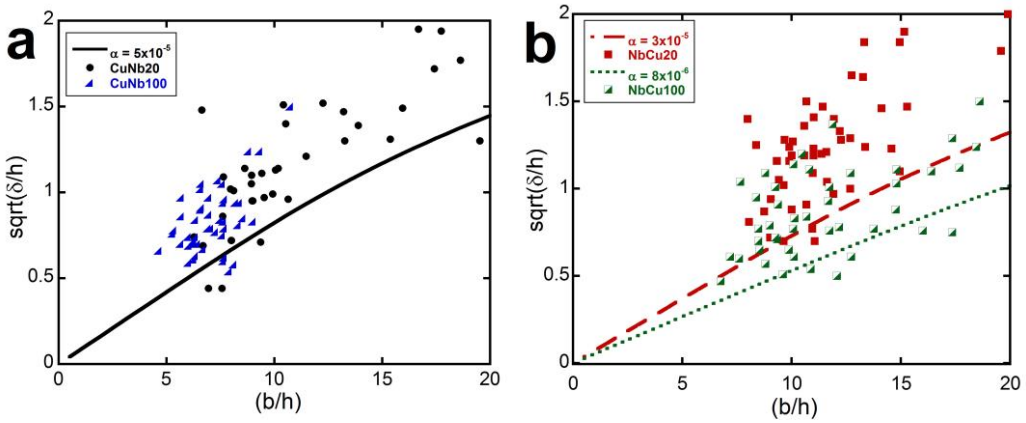

Figure 6: (a) The adhesion energy of the Cu-PI interface of the CuNb NMMs was found to be 10.7 Jm^{-2} using the minimum α value to fit the buckle data. (b) Two α values are necessary to determine the Nb-PI adhesion energy of the NbCu NMM. For the 20 nm layers 6.4 Jm^{-2} and for the 100 nm layers 1.5 Jm^{-2} were determined.

Table I: Film thicknesses, residual stresses, observed fracture and buckling strains, and calculated adhesion energies.

Film System	Total Film Thickness (nm)	Cu σ_{res} (MPa)	Nb σ_{res} (MPa)	Fracture Strain, ε_{frac} (%)	Buckling Strain, ε_{buck} (%)	Adhesion Energy, Γ (J/m^2)
CuNb20	925	936 ± 258	1389 ± 88	0.26 ± 0.03	3-4%	10.7 ± 2.1
CuNb100	925	202 ± 10	-480 ± 21	0.33 ± 0.08	5-6%	10.7 ± 2.1
NbCu20	950	1105 ± 81	1233 ± 127	0.4 ± 0.14	2.5-6%	6.4 ± 2.1
NbCu100	750	701 ± 24	-541 ± 115	0.51 ± 0.01	2-3.5%	1.5 ± 0.7

Conclusions

Cu/Nb NMMs on PI have been investigated using in-situ tensile straining with XRD and CLSM. With these two characterization techniques, the influence of layer thickness, layer order and residual stresses were examined. XRD provided information on the individual stresses in the Cu and Nb layers before and during straining, while the CLSM was used to quantify the crack density as a function of strain and the adhesion energy. The XRD experiments illustrated that the layer thickness influences the initial residual stresses and that thinner films can achieve higher stresses. The initial fracture strains did not differ for the different layer thicknesses or residual stresses. These results correlated well with the CLSM experiments with the layer order only having a small influence on the initial fracture strain and a significant impact on the measured interface adhesion. The layer thickness effect is the XRD data manifests in the increased saturation crack spacing where the 20 nm NMMs have the larger crack spacing. The residual stresses, especially in the 100 nm Nb layers (NbCu100, Nb100), affects the adhesion energy of the Nb-PI interface by decreasing the buckling strain and the measured adhesion energy (1.5 Jm^{-2}). The Cu-PI interface had a much higher adhesion energy (10.7 Jm^{-2}) which is in line with previous results of other ductile metals on PI. The results presented here illustrate that while NMMs may have good mechanical properties under compression (indentation or micro pillar compression), but under tension the fracture behavior is lacking. NMMs starting with a more ductile metal will tend to have better interfacial behavior compared to NMMs starting with a brittle metal. Finally, the residual stresses could be tailored to improve the mechanical behavior.

Acknowledgements

The authors would like to acknowledge Helmholtz Zentrum Berlin for the allocation of synchrotron radiation beam time and thankfully acknowledges the financial support of Helmholtz Zentrum Berlin (projects 14021169-ST, 15101992-ST, and 15202990-ST/R-1.1-P). Author D.R.E. would also like to acknowledge funding support from a 2014 Marshallplan Scholarship to conduct research at Montanuniversität Leoben.

References

[1] A. Misra, Mechanical behavior of metallic nanolaminates, in: Nanostructure Control Mater., 2006: pp. 146–176.

[2] A. Misra, J.P. Hirth, H. Kung, Single-dislocation-based strengthening mechanisms in nanoscale metallic multilayers, Philos. Mag. A. 82 (2002) 2935–2951. doi:10.1080/0l4l86102.

[3] E.O. Hall, The Deformation and ageing of mild steel: III discussion of results, Proc. Phys. Soc. B64 (1951) 747–753.

[4] N.J. Petch, The cleavage strength of polycrystals, J. Iron Steel Inst. London. 174 (1953) 25–28.

[5] J.D. Embury, R.M. Fischer, The structure and properties of drawn pearlite, Acta Metall. 14 (1966) 147–159.

[6] I.J. Beyerlein, N.A. Mara, J.S. Carpenter, T. Nizolek, W.M. Mook, T.A. Wynn, et al., Interface-driven microstructure development and ultra high strength of bulk nanostructured Cu-Nb multilayers fabricated by severe plastic deformation, J. Mater. Res. 28 (2013) 1799–1812. doi:10.1557/jmr.2013.21.

[7] Z. Farhat, Y. Ding, D. Northwood, A. Alpas, Nanoindentation and friction studies of Ti-based nanolaminated films, Surf. Coatings Technol. 89 (1997) 24–30. doi:10.1016/s0257-8972(96)02939-8.

[8] D.R. Economy, N.A. Mara, R.L. Schoeppner, B.M. Schultz, R.R. Unocic, M.S. Kennedy, Identifying Deformation and Strain Hardening Behaviors of Nanoscale Metallic Multilayers Through Nano-wear Testing, Metall. Mater. Trans. A Phys. Metall. Mater. Sci. 47 (2016) 1083–1095. doi:10.1007/s11661-015-3284-7.

[9] A.S.M.A. Haseeb, J.P. Celis, J.R. Roos, Fretting wear of metallic multilayer films, Thin Solid Films. 444 (2003) 199–207. doi:10.1016/S0040-6090(03)01089-7.

[10] N.A. Mara, A. Misra, R.G. Hoagland, A. V. Sergueeva, T. Tamayo, P. Dickerson, et al., High-temperature mechanical behavior/microstructure correlation of Cu/Nb nanoscale multilayers, Mater. Sci. Eng. A. 493 (2008) 274–282. doi:10.1016/j.msea.2007.08.089.

[11] A. Misra, M.J. Demkowicz, X. Zhang, R.G. Hoagland, The radiation damage tolerance of ultra-high strength nanolayered composites, JOM. 59 (2007) 62–65. doi:10.1007/s11837-007-0120-6.

[12] C.C. Aydiner, D.W. Brown, N.A. Mara, J. Almer, A. Misra, In situ x-ray investigation

of freestanding nanoscale Cu-Nb multilayers under tensile load, Appl. Phys. Lett. 94 (2009) 10–13. doi:10.1063/1.3074374.

[13] N.A. Mara, D. Bhattacharyya, R.G. Hoagland, A. Misra, Tensile behavior of 40 nm Cu/Nb nanoscale multilayers, Scr. Mater. 58 (2008) 874–877. doi:10.1016/j.scriptamat.2008.01.005.

[14] A. Misra, J.P. Hirth, R.G. Hoagland, Length-scale-dependent deformation mechanisms in incoherent metallic multilayered composites, Acta Mater. 53 (2005) 4817–4824. doi:10.1016/j.actamat.2005.06.025.

[15] H. Huang, F. Spaepen, Tensile testing of free-standing Cu, Ag, and Al thin films and Ag/Cu multilayers, Acta Mater. 48 (2000) 3261–3269. doi:10.1016/S1359-6454(00)00128-2.

[16] K. Wu, J.Y. Zhang, J. Li, Y.Q. Wang, G. Liu, J. Sun, Length-scale-dependent cracking and buckling behaviors of nanostructured Cu/Cr multilayer films on compliant substrates, Acta Mater. 100 (2015) 344–358. doi:10.1016/j.actamat.2015.08.055.

[17] K. Wu, J.Y. Zhang, G. Liu, P. Zhang, P.M. Cheng, J. Li, et al., Buckling behaviors and adhesion energy of nanostructured Cu/X (X = Nb, Zr) multilayer films on a compliant substrate, Acta Mater. 61 (2013) 7889–7903. doi:10.1016/j.actamat.2013.09.028.

[18] M. Wang, D. Wang, P. Schaaf, Size effect on the mechanical behavior of Al/Si multilayers deposited on Kapton substrate, J. Mater. Sci. Mater. Electron. 26 (2015) 8224–8228. doi:10.1007/s10854-015-3485-2.

[19] M.N. Polyakov, J. Lohmiller, P.A. Gruber, A.M. Hodge, Load Sharing Phenomena in Nanoscale Cu/Nb Multilayers, Adv. Eng. Mater. 15 (2014) 810–814. doi:10.1002/adem.201400368.

[20] V.M. Marx, F. Toth, A. Wiesinger, J. Berger, C. Kirchlechner, M.J. Cordill, et al., The influence of a brittle Cr interlayer on the deformation behavior of thin Cu films on flexible substrates: Experiment and model, Acta Mater. 89 (2015) 278–289. doi:10.1016/j.actamat.2015.01.047.

[21] B. Putz, R.L. Schoeppner, O. Glushko, D.F. Bahr, M.J. Cordill, Improved electro-mechanical performance of gold films on polyimide without adhesion layers, Scr. Mater. 102 (2015) 23–26. doi:10.1016/j.scriptamat.2015.02.005.

[22] S. Olliges, P.A. Gruber, S. Orso, V. Auzelyte, Y. Ekinci, H.H. Solak, et al., In situ observation of cracks in gold nano-interconnects on flexible substrates, Scr. Mater. 58 (2008) 175–178. doi:10.1016/j.scriptamat.2007.09.037.

[23] P.A. Gruber, E. Arzt, R. Spolenak, Brittle-to-ductile transition in ultrathin Ta/Cu film systems, J. Mater. Res. 24 (2009) 1906–1918. doi:10.1557/jmr.2009.0252.

[24] T. Jörg, M.J. Cordill, R. Franz, O. Glushko, J. Winkler, C. Mitterer, The electro-mechanical behavior of sputter-deposited Mo thin films on flexible substrates, Thin Solid Films. 606 (2016) 45–50. doi:10.1016/j.tsf.2016.03.032.

[25] M.J. Cordill, O. Glushko, B. Putz, Electro-Mechanical Testing of Conductive Materials Used in Flexible Electronics, Front. Mater. 3 (2016) 1–11. doi:10.3389/fmats.2016.00011.

[26] B. Putz, C. May-Miller, V. Matl, B. Völker, D.M. Többens, C. Semprimoschnig, et al., Two-stage cracking of metallic bi-layers on polymer substrates under tension, Scr. Mater. 145 (2018). doi:10.1016/j.scriptamat.2017.09.039.

[27] M.J. Cordill, O. Glushko, A. Kleinbichler, B. Putz, D.M. Többens, C. Kirchlechner, Microstructural influence on the cyclic electro-mechanical behaviour of ductile films on polymer substrates, Thin Solid Films. 644 (2017) 166–172. doi:10.1016/j.tsf.2017.06.067.

[28] M.J. Cordill, V.M. Marx, Fragmentation testing for ductile thin films on polymer substrates, Philos. Mag. Lett. 93 (2013). doi:10.1080/09500839.2013.830792.

[29] M.J. Cordill, F.D. Fischer, F.G. Rammerstorfer, G. Dehm, Adhesion energies of Cr thin films on polyimide determined from buckling: Experiment and model, Acta Mater. 58 (2010). doi:10.1016/j.actamat.2010.06.032.

[30] B. Putz, G. Milassin, Y. Butenko, B. Völker, C. Gammer, C. Semprimoschnig, et al., Combined TEM and XPS studies of metal - polymer interfaces for space applications, Surf. Coatings Technol. 332 (2017) 368–375. doi:10.1016/j.surfcoat.2017.07.079.

[31] D.R. Economy, B.M. Schultz, M.S. Kennedy, Impacts of accelerated aging on the mechanical properties of Cu-Nb nanolaminates, J. Mater. Sci. 47 (2012) 6986–6991. doi:10.1007/s10853-012-6649-y.

[32] D. Többens, S. Zander, KMC-2 : an X-ray beamline with dedicated di raction and XAS

endstations at BESSY II, J. Large-Scale Res. Facil. 2 (2016) 1–6.

[33] L. Spieß, G. Teichert, R. Schwarzer, H. Behnken, C. Genzel, Moderne röntgenbeugung, Teubner, Wiesbad. (2005).

[34] I.C. Noyan, J.B. Cohen, Residual stress: measurement by diffraction and interpretation, Springer-Verlag, New York, 2013.

[35] H. Wern, N. Koch, T. Maas, Selfconsistent calculation of the x-ray elastic constants of polycrystalline materials for arbitrary crystal symmetry, in: Mater. Sci. Forum, 2002: pp. 127–132. http://www.scopus.com/inward/record.url?eid=2-s2.0-0036433960&partnerID=tZOtx3y1.

[36] T. Jörg, M.J. Cordill, R. Franz, C. Kirchlechner, D.M. Többens, J. Winkler, et al., Thickness dependence of the electro-mechanical response of sputter-deposited Mo thin films on polyimide: Insights from in situ synchrotron diffraction tensile tests, Mater. Sci. Eng. A. 697 (2017) 17–23. doi:10.1016/j.msea.2017.04.101.

[37] B. Putz, O. Glushko, V.M. Marx, C. Kirchlechner, D. Többens, M.J. Cordill, Electro-mechanical performance of thin gold films on polyimide Barbara, MRS Adv. 1 (2016) 773–778. doi:https://doi.org/10.1557/adv.2016.233.

[38] M.J. Cordill, A.A. Taylor, J. Berger, K. Schmidegg, G. Dehm, Robust mechanical performance of chromium-coated polyethylene terephthalate over a broad range of conditions, Philos. Mag. 92 (2012). doi:10.1080/14786435.2012.700418.

[39] M.J. Cordill, A. Taylor, J. Schalko, G. Dehm, Fracture and delamination of chromium thin films on polymer substrates, Metall. Mater. Trans. A Phys. Metall. Mater. Sci. 41 (2010). doi:10.1007/s11661-009-9988-9.

[40] M.J. Cordill, A.A. Taylor, Thickness effect on the fracture and delamination of titanium films, Thin Solid Films. 589 (2015) 209–214. doi:10.1016/j.tsf.2015.05.021.

[41] V.M. Marx, M.J. Cordill, D.M. Többens, C. Kirchlechner, G. Dehm, Effect of annealing on the size dependent deformation behavior of thin cobalt films on flexible substrates, Thin Solid Films. 624 (2017). doi:10.1016/j.tsf.2017.01.011.

[42] J.M. Burkstrand, Metal-polymer interfaces: Adhesion and x-ray photoemission studies, J. Appl. Phys. 52 (1981) 4795–4800. doi:10.1063/1.329320.

[43] M.J. Cordill, F.D. Fischer, F.G. Rammerstorfer, G. Dehm, Adhesion energies of Cr

thin films on polyimide determined from buckling: Experiment and model, Acta Mater. 58 (2010) 5520–5531. doi:10.1016/j.actamat.2010.06.032.

[44] F. Toth, F.G. Rammerstorfer, M.J. Cordill, F.D. Fischer, Detailed modelling of delamination buckling of thin films under global tension, Acta Mater. 61 (2013). doi:10.1016/j.actamat.2013.01.014.

[45] V.M. Marx, C. Kirchlechner, I. Zizak, M.J. Cordill, G. Dehm, Adhesion measurement of a buried Cr interlayer on polyimide, Philos. Mag. 95 (2015) 1982–1991. doi:10.1080/14786435.2014.920543.

[46] T. Jörg, M.J. Cordill, R. Franz, C. Kirchlechner, D.M. Többens, J. Winkler, et al., Thickness dependence of the electro-mechanical response of sputter-deposited Mo thin films on polyimide: Insights from in situ synchrotron diffraction tensile tests, Mater. Sci. Eng. A. 697 (2017) 17–23. doi:10.1016/j.msea.2017.04.101.

[47] M.J. Cordill, V.M. Marx, C. Kirchlechner, Ductile film delamination from compliant substrates using hard overlayers, Thin Solid Films. 571 (2014) 302–307. doi:10.1016/j.tsf.2014.02.093.